Mechanical Properties of a β-Type Titanium Alloy Cast Using a Calcia Mold for Biomedical Applications

著者	Tsutsumi Harumi, Niinomi Mitsuo, Akahori Toshikazu, Nakai Masaaki, Takeuchi Tsutomu, Katsura Shigeki
journal or publication title	Materials Transactions
volume	51
number	1
page range	136-142
year	2010
URL	http://hdl.handle.net/10097/52149

Materials Transactions, Vol. 51, No. 1 (2010) pp. 136 to 142

Mechanical Properties of a β-Type Titanium Alloy Cast Using a Calcia Mold for Biomedical Applications

Harumi Tsutsumi[1], Mitsuo Niinomi[1], Toshikazu Akahori[1], Masaaki Nakai[1], Tsutomu Takeuchi[2] and Shigeki Katsura[3]

[1]*Institute for Materials Research, Tohoku University, Sendai 980-8577, Japan*
[2]*Takeuchi Katan, Ltd., Toyohashi 441-8132, Japan*
[3]*Yamahachi Dental Mgf., Co., Gamagori 443-0105, Japan*

A calcia mold, which is stable at high temperatures for dental precision casting of β-type titanium alloys such as Ti-29Nb-13Ta-4.6Zr (TNTZ) with high melting point, has been developed. The applicability of the calcia mold to casting TNTZ was evaluated with focusing on the mechanical properties of the casting in this study. The molten TNTZ was cast into the calcia mold of which dimensional accuracy was controlled by adding pure zirconium particles. The tensile and fatigue properties of TNTZ cast into the calcia mold were examined with comparing those of TNTZ cast into the magnesia mold, which is the conventional one for casting titanium alloys.

The tensile properties of TNTZ cast into the calcia and the magnesia molds are not markedly different. The fatigue strength of TNTZ cast into the calcia mold in the low- and high-cycle fatigue life regions is slightly higher than that of TNTZ cast into the magnesia mold. Therefore, the calcia mold is expected to be applicable to the dental precision casting of TNTZ. [doi:10.2320/matertrans.L-M2009828]

(Received June 19, 2009; Accepted August 26, 2009; Published December 25, 2009)

Keywords: *β-type titanium alloy, dental precision casting, calcia mold, magnesia mold, tensile properties, fatigue properties*

1. Introduction

A demand of a dental precision casting of the titanium (Ti) alloys has increased because of their high corrosion resistance and high mechanical properties.[1–3] For example, a Ti-29Nb-13Ta-4.6Zr (TNTZ) alloy composed of non-toxic and non-allergenic elements has been predicted to be the next-generation biomaterial for prosthetic appliances and dental implants.[4–8] However conventional investment materials aren't sometimes suitable for the dental precision casting of Ti alloys because the melting point of some Ti alloys are much higher than that of a conventional Ti alloy, Ti-6Al-4V ELI. Therefore, development of investment materials that are stable at high temperatures is highly required.

Authors have focused on calcia particles as heat-resistant investments.[9,10] Calcia particles are among the most stable oxides in terms of the free energy of formation, thus, inhibition of the interface reaction is expected.[11–13] In our previous study, the surface of the calcia mold fabricated with a mixture of fine (diameter < 0.3 mm) and coarse (diameter $= 1$–3 mm) calcia particles was smooth and showed no cracks or defects.[9] The surface of the TNTZ cast using the duplex-coated wax pattern with the fine pure calcia slurry and crushed silica fiber-reinforced fine calcia slurry were very fine without penetration.[9] In addition, dimensional accuracy of calcia mold and cast TNTZ could be controlled by adding zirconium particles to calcia mold.[10] Moreover the surface reaction layer and volume fraction of casting defects were restrained to a larger extent by casting into the calcia mold than into the magnesia mold, which is a conventional investment mold for casting titanium alloys.[10] These results indicate that the calcia mold is suitable for the dental precision casting of TNTZ. However, the mechanical properties of the cast TNTZ using duplex-coated calcia mold are not yet clearly understood. Investigating the mechanical properties of the TNTZ cast using calcia mold is also needed in to evaluate the applicability of the dental precision casting technique using the calcia mold for TNTZ. Therefore, the mechanical properties of the TNTZ cast using the calcia mold were investigated with comparing those of the TNTZ cast using the conventional magnesia mold in this study.

2. Materials and Methods

2.1 Materials

TNTZ disks with a diameter of 30 mm and a thickness of 13 mm were prepared from a hot forged TNTZ bar (Nb: 29.2 mass%, Ta: 12.2 mass%, Zr: 4.3 mass%, Fe: 0.05 mass%, N: 0.04 mass%, O: 0.01 mass% and Ti: balance) with a diameter of 30 mm and a length of 1000 mm.

2.2 Wax pattern

A dog-bone-type wax pattern was formed using commercially available paraffin wax. Schematic drawings of the dog-bone-type wax pattern for tensile and fatigue is shown in Fig. 1. Sprue and a sprue runner were set in the wax patterns as shown in Fig. 1. Several wax patterns were coated with a calcia slurry to obtain a smooth casting surface, as described in detail below.

2.3 Mold

Two different sizes of electrically fused calcia particles with diameters below 0.3 mm (C_1) and 1–3 mm (C_2) were used in this study. The chemical composition of the magnesia-based investment (hereafter magnesia investment) is shown in Table 1. The bonding agent of the investment used in this study was a methanol solution with 7 mass% calcia chloride, $CaCl_2$. C_1 particles were mixed with the bonding agent at a ratio of 4 : 1 by weight, and a C_1 slurry

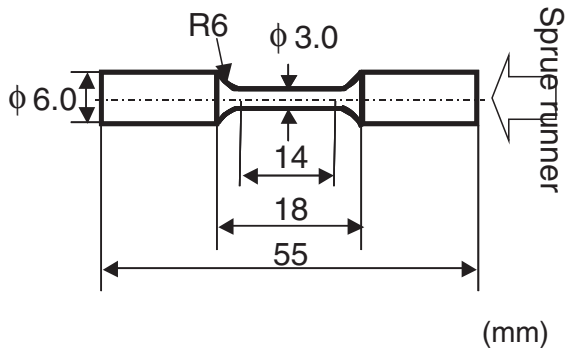

Fig. 1 Schematic drawing of the wax pattern for tensile and fatigue test specimens.

Table 1 Chemical compositions of electrically fused calcia (a) and magnesia-based investment (b).

(a) Electrically fused calsia (mass%)

MgO	SiO_2	Al_2O_3	Fe_2O_3	CaO
0.67	0.43	0.02	0.02	bal.

(b) Magnesia-based investment (mass%)

SiO_2	Na_2O	Fe_2O_3	Al_2O_3	MgO
1.64	0.59	0.55	0.37	bal.

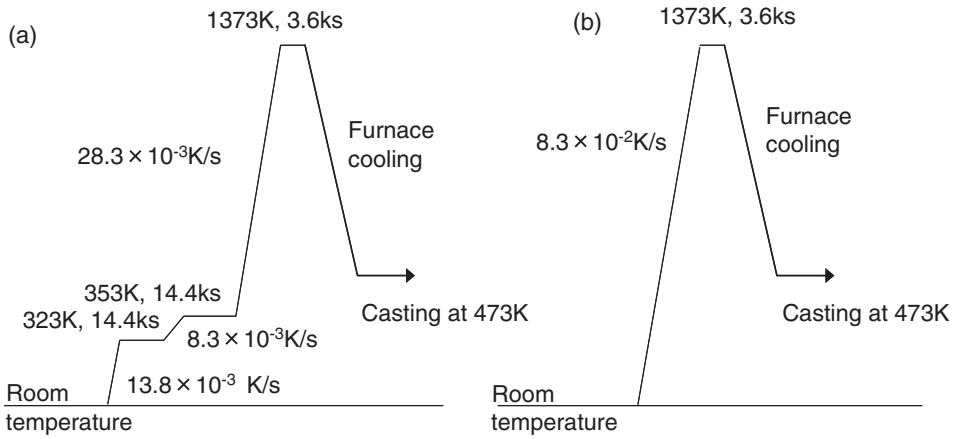

Fig. 2 Schematic drawings of the multiple baking processes for the calcia (a) and magnesia (b) molds.

was obtained (slurry A). Then, 0.3 mass% silica fiber meshes ($5 \times 5\,mm^2$, 2 mm in thickness) and 12 mass% 45-μm pure zirconium particles (used as expansive components) were mixed into slurry A (slurry B). Wax patterns were immersed in slurry A and subsequently in slurry B. In order to avoid mixed calcia particles, the wax patterns were coated at 1.2 ks intervals. Mixture calcia particles of 40%C_1 and 60%C_3 by weight were used as the investment material. The mixed calcia particles were further mixed with the bonding agent at a ratio of 93 (calcia particles): 7 (bonding agent) by weight and then invested in a mold frame with the wax pattern obtained with the calcia slurry coatings A mold frame with a diameter of 70 mm and a length of 100 mm was used. The invested molds were held in a vacuum desiccator (0.06×10^{-6} Pa) for 86.4 ks at room temperature. Multiple baking processes were then carried out with the molds using an electrical muffle furnace. A schematic image of the multiple baking processes for the calcia mold is shown in Fig. 2(a).

A commercially available magnesia-based investment with alumina cement was also used as a control. The chemical composition of the magnesia investment is shown in Table 1. The magnesia investment was mixed with distilled water at a ratio of 100 (magnesia investment): 13 (distilled water) by weight and then invested in a mold frame with the untreated wax patterns. The invested molds were dried in air for 3.6 ks and baked at 1373 K for 3.6 ks (Fig. 2(b)). Hereafter the calcia and magnesia molds will be called $mold_{calcia}$ and $mold_{megnaseia}$, respectively.

2.4 Casting

Casting of the TNTZ was carried out using an argon pressure-type dental precision casting machine. The TNTZ disks were melted for 50 s under 10.2×10^{-6} Pa by a 300-A mono arc and then cast under 0.7 MPa argon pressure using the calcia and the magnesia molds as described above (hereafter the TNTZ cast using the $mold_{calcia}$ and $mold_{magnesia}$ will be called $TNTZ_{calcia}$ and $TNTZ_{magnesia}$, respectively).

2.5 Tensile test

Tensile tests of the cast TNTZ were carried out. Before testing, only $TNTZ_{magnesia}$ was sandblasted to remove the thick surface reaction layer. ($TNTZ_{calcia}$ was not need to sandblast.) Tensile tests were carried out using an instron-type testing machine having a capacity of 9.8 kN at a crosshead speed of $8.33 \times 10^{-6}\,m \cdot s^{-1}$ at room temperature. A load was detected using a load cell of the testing machine. The elongation was measured using a strain gauge directly attached to the cast TNTZ. The fractured surface of the cast TNTZ was observed using a scanning electron microscopy (SEM). The area of shrinkages occupying the fractured surface was measured. The volume fraction of shrinkage, V, was calculated by the following

$$V = D/A, \tag{1}$$

where D and A are the area of shrinkages, total area, respectively. In order to distinguish cast defects from dimples, only cast defects over 10 μm were evaluated.

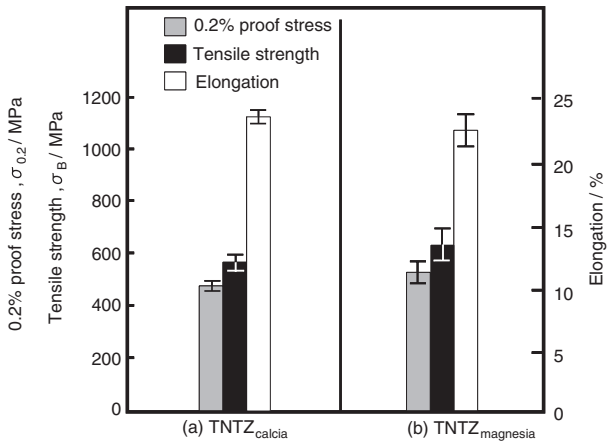

Fig. 3 Tensile properties of the $TNTZ_{calcia}$ (a) and $TNTZ_{magnesia}$ (b).

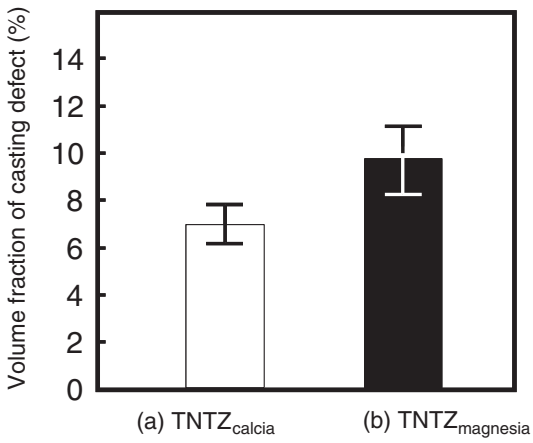

Fig. 5 Volume fractions of the casting defects on the tensile facture surfaces of the $TNTZ_{calcia}$ (a) and $TNTZ_{magnesia}$ (b).

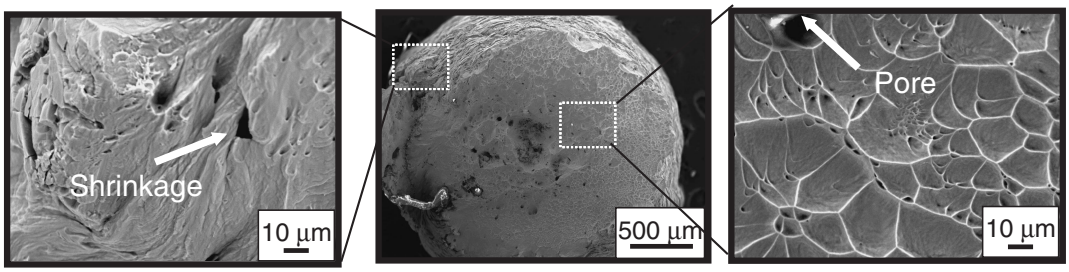

Fig. 4 SEM fractographs of the $TNTZ_{calcia}$ after the tensile test.

2.6 Fatigue test

Fatigue tests of the cast TNTZ were carried using an electro-servo-hydraulic machine. Each fatigue test was performed at a frequency of 10 Hz with a stress ratio, $R = 0.1$, under the tension-tension mode in air at room temperature. The maximum cycle stress at which a specimen was still unfailing at 10^7 cycles was defined as the fatigue limit in this study. The fractured surface of the cast TNTZ was observed using an SEM, and the volume fraction of the casting defects was calculated. In order to distinguish cast defects from dimples, only cast defects over 10 μm were evaluated.

3. Results and Discussion

3.1 Tensile properties of cast TNTZ

Figure 3 shows the tensile properties of the $TNTZ_{calcia}$ and $TNTZ_{magnesia}$. Mechanical properties of the $TNTZ_{calcia}$, i.e., the tensile strength, the 0.2% proof strength and the elongation, are almost the same as those of the $TNTZ_{magnesia}$. However, the error bar of the mechanical properties of the $TNTZ_{calcia}$ (around 5%) is smaller than that of the $TNTZ_{magnesia}$ (around 10%). The tensile strength and elongation of the Au-Ag-Pd alloy, which is a conventional dental cast alloy, are 400–600 MPa and 10–40%, respectively.[14] Therefore, the mechanical properties of the $TNTZ_{calcia}$ are the achieved properties of a conventional cast alloy, and the $TNTZ_{calcia}$ can be used as a dental cast alloy.

Figure 4 shows the SEM fractographs of the $TNTZ_{calcia}$ after a tensile test. A ductile fracture surface with dimples is observed on the $TNTZ_{calcia}$, and the average diameter of the dimple at the fracture surface is over 10 μm. In addition, a brittle fractured surface with cleavage facets is observed at a surface reaction layer of the $TNTZ_{calcia}$. Casting defects, such as shrinkage and the appearance of pores, are observed on the fracture surface. The volume fraction of the casting defects on the tensile facture surface of the $TNTZ_{calcia}$ and $TNTZ_{magnesia}$ is shown in Fig. 5. The volume fraction of the casting defects of the $TNTZ_{calcia}$ is lower than that of the $TNTZ_{magnesia}$. Figure 6 shows the distribution of casting defects on the tensile fracture surface of the $TNTZ_{calcia}$ and $TNTZ_{magnesia}$. Number and distribution of diameter of the casting defects at the $TNTZ_{calcia}$ are smaller than those of the $TNTZ_{magnesia}$. Casting defects over 40 μm (large casting defects) are observed on the fracture surface of the $TNTZ_{calcia}$ and $TNTZ_{magnesia}$. These large casting defects are not observed at the cross section of the $TNTZ_{calcia}$ and $TNTZ_{magnesia}$ before the tensile test. Cracks are believed to initiate from casting defects. Stress concentration occurs at the site of the casting defects and casting defects become bigger. TNTZ is fractured through a large casting defect that serves as a crack initiation area.

The relationship between the tensile strength and volume fraction of casting defects on the cross section of the $TNTZ_{calcia}$ and $TNTZ_{magnesia}$ is shown in Fig. 7. In spite of the increasing volume faction of casting defects, the tensile strength of the $TNTZ_{calcia}$ is almost the same. On the other hand, the tensile properties of the $TNTZ_{magnesia}$ decreased with an increase in the volume fraction of casting defects. Dispersion of the tensile properties of the $TNTZ_{calcia}$ is

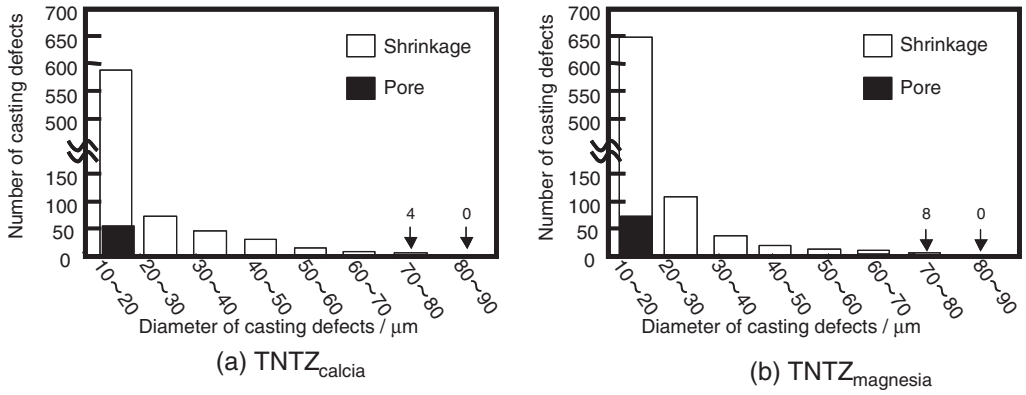

Fig. 6 Distributions of casting defects on the tensile fracture surface of the $TNTZ_{calcia}$ (a) and $TNTZ_{magnesia}$ (b).

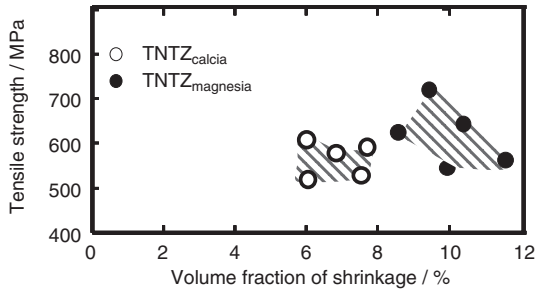

Fig. 7 Relationships between the tensile strength and the volume fraction of casting defects on the cross sections of the $TNTZ_{calcia}$ and $TNTZ_{magnesia}$.

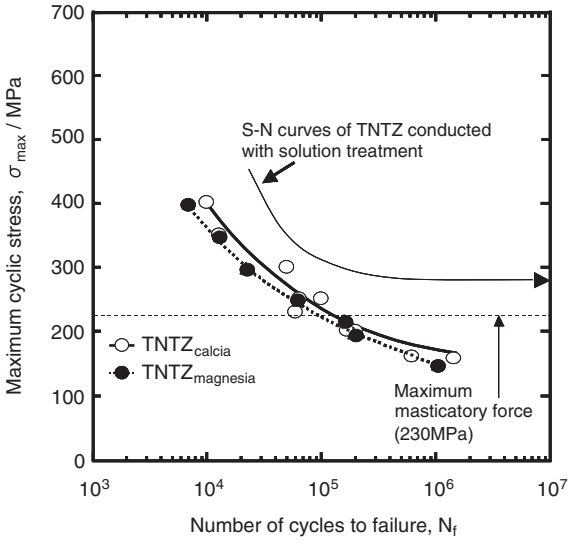

Fig. 8 S-N curves of the $TNTZ_{calcia}$, $TNTZ_{magnesia}$, and forged TNTZ solutionized at 1063 K for 3.6 ks obtained from fatigue tests.

considered to be smaller than that of the $TNTZ_{magnesia}$, since the number and distribution of diameter of the casting defects at the $TNTZ_{calcia}$ are smaller than those of the $TNTZ_{magnesia}$.

3.2 Fatigue properties of cast TNTZ

The S-N curves obtained from fatigue tests on the $TNTZ_{calcia}$, the $TNTZ_{magnesia}$, and forged TNTZ solutionized at 1063 K for 3.6 ks are shown in Fig. 8.[15] Maximum masticatory stress is also shown in the same figure for comparison.[16] The fatigue strength of the $TNTZ_{calcia}$ is slightly higher than that of the $TNTZ_{magnesia}$ in both the low-cycle-fatigue life region, where the number of cycles to failure is less than 10^4 cycles, and the high-cycle-fatigue life region, where the number of cycles to failure exceeds 10^5 cycles. While exact fatigue limits cannot be obtained, the fatigue limits of the $TNTZ_{calcia}$ and $TNTZ_{magnesia}$ are estimated to be almost 150 MPa and 140 MPa, respectively. Therefore, the fatigue limit of the $TNTZ_{calcia}$ is lower than that of the forged TNTZ (almost 280 MPa). Because cast TNTZ has many casting defects and a dendritic structure, its resistance to fatigue crack initiation is small. As a result, the fatigue limit of cast TNTZ is lower than that of the forged TNTZ. Typical SEM fractographs of the $TNTZ_{calcia}$ and $TNTZ_{magnesia}$ in the low- and high-cycle-fatigue life regions after fatigue tests are shown in Fig. 9 and Fig. 10. Fatigue cracks tend to initiate from the surface of the $TNTZ_{calcia}$ and $TNTZ_{magnesia}$ in the low-cycle-fatigue life region. The crack initiation sites are, almost always, casting defects or α-case at the surface. In addition, the fatigue strength of cast TNTZ seemed to decrease when a fatigue crack was initiated from casting defects. Striations are observed on the stable fracture surface, and equiaxed dimples are observed on the fast fracture surface. Fatigue cracks tended to initiate from the casting defect on the inside of the $TNTZ_{calcia}$ and $TNTZ_{magnesia}$ in the high-cycle-fatigue life region. In this case, striations were observed on the stable fracture, and equiaxed dimples were observed on the fast fracture surface. In addition, the interval of striations in the high-cycle-fatigue life regions was narrower than that in the low-cycle-fatigue life region. It is commonly believed that fatigue strength depends on the surface roughness of a material. However, the main crack initiation sites of cast TNTZ are casting defects on the surface or the inside of cast TNTZ. Stress concentration is easily generated from a casting defect rather than on the surface of the cast TNTZ because casting defects are large, even though cracks also initiate on the surface of cast TNTZ. Therefore, it is considered that the fatigue strength of cast TNTZ strongly depends on casting defects.

Figure 11 shows the volume fraction of the casting defects on a fatigue fracture surface of the $TNTZ_{calcia}$ and $TNTZ_{magnesia}$ in the low-cycle-fatigue life region. The volume fraction of the casting defects on the fatigue fracture

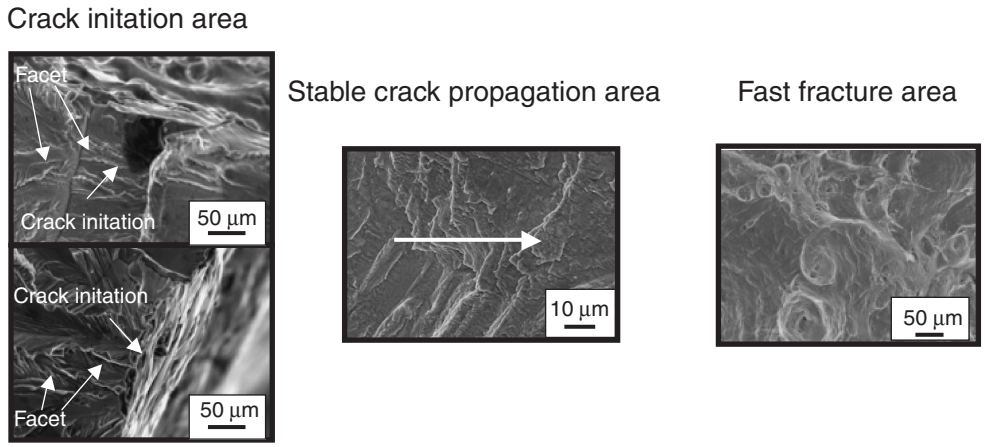

(a) Low-cycle fatigue life region (σ_{max} = 350MPa)

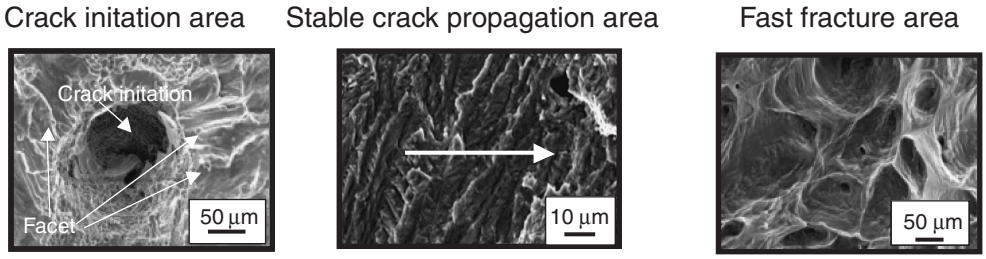

(b) High-cycle fatigue life region (σ_{max} = 160MPa)

Fig. 9 Typical SEM fractographs of the $TNTZ_{calcia}$ in low- (a) and high- (b) cycle-fatigue life regions after fatigue tests.

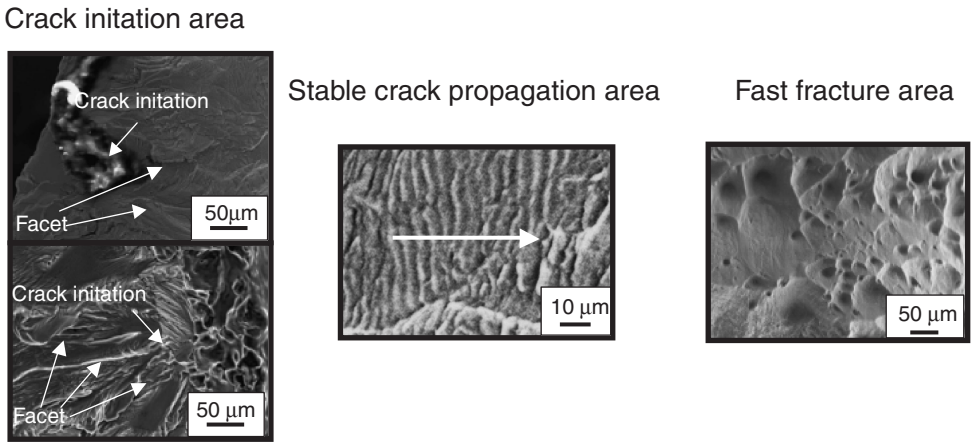

(a) Low-cycle fatigue life region (σ_{max} = 300MPa)

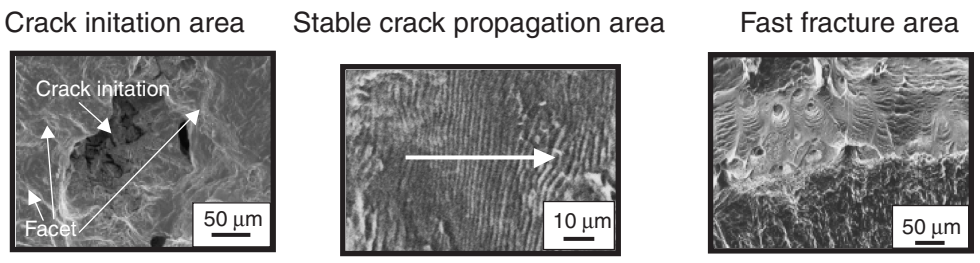

(b) High-cycle fatigue life region (σ_{max} = 150MPa)

Fig. 10 Typical SEM fractographs of the $TNTZ_{magnesia}$ in low- (a) and high- (b) cycle-fatigue life regions after fatigue tests.

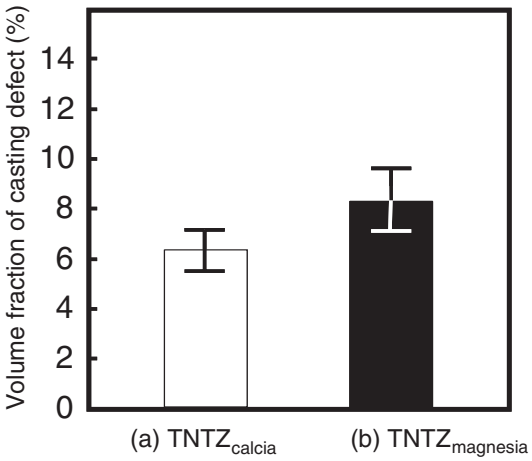

Fig. 11 Volume fractions of casting defects on the fatigue fracture surface of the $TNTZ_{calcia}$ (a) and $TNTZ_{magnesia}$ (b) in the low-cycle-fatigue life region.

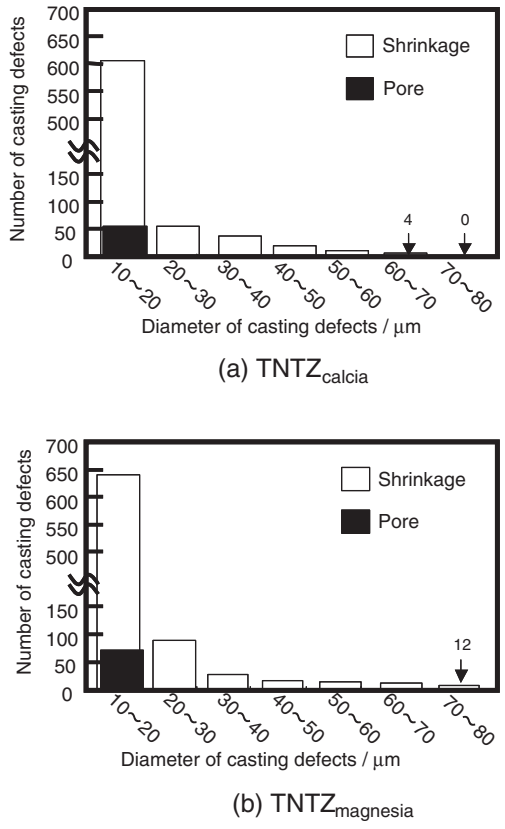

Fig. 12 Distributions of the casting defects on the fatigue fracture surfaces of the $TNTZ_{calcia}$ (a) and $TNTZ_{magnesia}$ (b) in the low-cycle-fatigue life region.

surface of the $TNTZ_{calcia}$ is 2–3% lower than that of the $TNTZ_{magnesia}$. Figure 12 shows the distribution of casting defects on the fatigue fracture surface of $TNTZ_{calcia}$ and $TNTZ_{magnesia}$ in the low-cycle-fatigue life region. Casting defects over 60 μm are observed on the fracture surface of the $TNTZ_{calcia}$ and $TNTZ_{magnesia}$. More coarse defects are present in this case than in a cross section of the $TNTZ_{calcia}$ before fatigue test because a crack propagates through large casting defects during the fatigue test. In addition, the maximum diameter of casting defects of the $TNTZ_{calcia}$ and $TNTZ_{magnesia}$ is 70 μm and 80 μm, respectively. The number and distribution of the diameter of casting defects in the $TNTZ_{calcia}$ are smaller than those in the $TNTZ_{magnesia}$. Since resistance to fatigue crack initiation is higher in the $TNTZ_{calcia}$ than in the $TNTZ_{magnesia}$, the fatigue strength of the $TNTZ_{calcia}$ is considered to be higher than that of the $TNTZ_{magnesia}$ in the low-cycle-fatigue life region.

In general, masticatory stress is said to be 20–230 MPa during a meal[15] and the estimated fatigue limit of $TNTZ_{calcia}$ is lower than that of this masticatory force. Therefore, improved fatigue strength of the $TNTZ_{calcia}$ is required for dental prosthetic appliances. Casting defects are dominant factors of fatigue properties, as described above. Therefore, improvement of fatigue strength is anticipated with the inhibition of casting defects. In addition, the fatigue strength of forged TNTZ is improved by heat treatment.[16] Therefore, an improvement of fatigue strength of the $TNTZ_{calcia}$ is also anticipated with the use of heat treatments.

4. Conclusions

The mechanical properties of the TNTZ for biomedical applications cast using the calcia mold were investigated in this study. The following results were obtained.

(1) The difference in the tensile properties between the $TNTZ_{calcia}$ and $TNTZ_{magnesia}$ is very small.

(2) The fatigue strength of $TNTZ_{calcia}$ in the low- and high-cycle-fatigue life regions is slightly higher than that of $TNTZ_{magnesia}$.

Acknowledgements

This work was supported in part by a Grant-in-Aid for Young Scientists (21760549), MEXT (Tokyo, Japan); the Global COE Materials Integration Program (International Center of Education and Research), Tohoku University; MEXT (Tokyo, Japan); R&D Institute of Metals and Composites for Future Industries (Tokyo, Japan); Interuniversity Cooperative Research Program of the Advanced Research Center of Metallic Glasses, Institute for Materials Research, Tohoku University (Sendai, Japan); Interuniversity Cooperative Research Program of the Institute for Materials Research, Tohoku University (Sendai, Japan); the Light Metal Educational Foundation (Osaka, Japan); and the project between Tohoku University and Kyusyu University on “Highly-functional Interface Science: Innovation of Biomaterials with Highly functional Interface to Host and Parasite,” MEXT (Tokyo, Japan).

REFERENCES

1) K. Ida and I. Miura: *Application of Titanium for Denture Field*, (1998) pp. 11–14.
2) Y. Okazaki, A. Ito, T. Tateishi and Y. Ito: J. Japan Inst. Metals **57** (1993) 332–337.
3) T. Hanwa: J. Jpn. Soc. Biomat. **23** (2005) 83–90.
4) M. Niinomi, T. Hattori, K. Morikawa, T. Kasuga, A. Suzuki, H. Fukui and S. Niwa: Mater. Trans. **43** (2002) 2970–2977.
5) M. Niinomi: Biomaterials **24** (2003) 2673–2683.

6) Y. L. Hao, M. Niinomi, D. Kuroda, K. Fukunaga, R. Yang and A. Suzuki: Metall. Mater. Trans. A **34** (2003) 1007.
7) S. J. Li, M. Niinomi, T. Akahori, T. Kasuga, R. Yang and Y. L. Hao: Biomaterials **25** (2004) 3341–3349.
8) M. Niinomi, T. Akahori, T. Manabe, T. Takeuchi, S. Katsura, H. Fukui and A. Suzuki: Tetsu-to-Hagane **90** (2004) 154.
9) H. Tsutsumi, M. Niinomi, T. Akahori, M. Nakai, T. Takeuchi and S. Katsura: Mater. Trans. **50** (2009) 2057–2063.
10) H. Tsutsumi, M. Niinomi, T. Akahori, M. Nakai, T. Takeuchi and S. Katsura: Mater. Trans. **51** (2010) 128–135.
11) A. Sato, N. Matsumoto, Y. Yoneda, T. Takahashi and H. Iwanabe: Imono **14** (1990) 244–253.
12) M. G. Kim, S. K. Kim and Y. J. Kim: Mater. Trans. **43** (2002) 745–750.
13) Y. Tamaoki and T. Miyazaki: Prosthodont. Res. Pract. **42** (1998) 528–534.
14) *Japanese Industrial Standards*, Dental Casting Gold-Silver-Palladium Alloy, T6106, (1985).
15) T. Akahori, M. Niinomi, H. Fukui and A. Suzuki: Mater. Trans. **45** (2004) 1540–1548.
16) T. Minamoto, M. Niinomi, T. Akahori, Y. Nakano and H. Fukui: J. J. Dent. Mater. **22** (2003) 210–220.